PD-L1+ Neutrophils mediate Susceptibility during Systemic Inflammatory Response in Non-Alcoholic Fatty Liver Disease

Cleyson da Cruz Oliveira Barros[1,2], Alexandre Kanashiro[1,2], Gabriel Victor Lucena da Silva[1,2], Guilherme Cesar Martelossi Cebinelli[1,2], Luiz Osório Leiria[1,2], Thiago Mattar Cunha[1,2], José Carlos Alves Filho[1,2], and Fernando Queiroz Cunha[1,2]

[1]Center for Research in Inflammatory Diseases (CRID), Ribeirão Preto Medical School, University of São Paulo, Av. Bandeirantes; Rua das Paineiras, Casa 3, Ribeirão Preto, São Paulo, 14049-900, Brazil.

[2]Department of Pharmacology, Ribeirão Preto Medical School, University of São Paulo, Ribeirão Preto, São Paulo, Brazil.

e-mail: fqdcunha@fmrp.usp.br

Abstract

Non-alcoholic fatty liver disease (NAFLD) is a pathological condition affecting individuals worldwide. Patients with NAFLD are more susceptible to systemic inflammation, such as sepsis, which accelerates liver damage. However, the immunological mechanisms that trigger the hyper-inflammatory responses in individuals with NAFLD remain unknown. In the present study, we reported that short-term HFCD (Choline Deficient High Fat Diet)-fed mice, which did not show significative signs of hepatic damage and inflammation in the first two weeks, are more susceptible to mortality after lipopolysaccharide (LPS) challenge. Mechanistically, endotoxemic mice show an excessive accumulation of NK-producing IFN-γ cells in liver tissue triggering the recruitment and polarization of a distinct neutrophil subset, characterized by high PD-L1 expression and massive TNFα production. Remarkably, genetic inhibition of IFN-γ or pharmacological blockade of PD-L1 effectively modulated the excessive recruitment of these neutrophils to the liver and TNFα release, thereby preventing hepatic damage and reducing the severity of host mortality. Thus, these results support the design of novel effective strategies to control hyperinflammatory responses in patients with HFCDs and consequently prevent hepatic damage and mortality..

Key Words: neutrophil; NAFLD; endotoxemia; PDL-1.

1. INTRODUCTION

Non-alcoholic fatty liver disease (NAFLD) is a metabolic hepatic dysfunction defined as an abnormal accumulation of fat within the liver without secondary triggers such as alcohol consumption. NAFLD has become a common chronic liver disease in the world population and has a high prevalence varying from simple steatosis to non-alcoholic steatohepatitis, fibrosis, cirrhosis, and hepatocellular carcinoma (1–3). Despite its high prevalence and increasing cause of liver-related mortality worldwide, NAFLD is still underestimated, and there are no approved pharmacological or preventive strategies for these medical conditions(4, 5).

The NAFLD is highly complex and involves a “multi-hit” process in which different stimuli act together to promote fat accumulation and progressive liver damage(6). Although the pathogenesis of NAFLD is multifactorial, inflammation has now been considered a key factor in the progression of advanced hepatic conditions(7–9). In the presence of obesity and lipotoxicity, the immune system is activated in the liver, with a corresponding degree of inflammation triggered by the “wound healing response”. Since these inflammatory signs persist for a long period, monocytes and neutrophils, as well as T CD4, T CD8, and natural killer (NK), can be recruited to the liver, releasing a massive quantity of pro-inflammatory cytokines, mainly interferon-gamma (IFN-γ) and tumor necrosis factor (TNFα)(7, 10). Likewise in autoimmune diseases, these cytokines are also present in systemic and uncontrolled inflammatory processes, such as sepsis(11). Sepsis is a syndrome characterized by a life-threatening dysfunction due to complex interactions between pathogens and the host recruitment of immune cells, resulting in a systemic hyper-inflammatory state followed by extensive vital organ damage, including in the liver(12, 13). Sepsis has also been considered the leading cause of death in intensive care units. In endotoxemia, rodents develop a sepsis-like inflammatory response, characterized by a massive production of cytokines that provokes uncontrolled recruitment of innate immune cells, mainly monocytes, and neutrophils to vital organs, such as the liver, inducing extensive and lethal damage(11, 14, 15). The majority of data regarding endotoxemia pathogenesis have focused only on the interaction between the infection and the host immune system, and only a few studies have addressed one or more clinical conditions that are considered risk factors leading to endotoxemia aggravation, such as senescence and previous immunosuppressive comorbidities(16–18). Thus,

understanding how these clinical conditions can modify the host immune response and consequently affect the outcome of sepsis is crucial to detecting the risks and designing novel preventive and therapeutic approaches to control exacerbated inflammatory responses. Recently, some populational studies, including large-scale data from cohorts with biopsy-confirmed individuals, have evidenced a higher incidence of severe infections in NAFLD patients, suggesting that previous hepatic conditions can modify the host immune response, leading to sepsis aggravation(19). However, although a relationship between elevated risk of sepsis in NAFLD patients exists, the underlying immunological mechanisms involved in the progression and exacerbation of systemic and local (hepatic) inflammation in these individuals have not been identified yet.

To understand the impact of NAFLD on liver damage during endotoxemia, we used a known murine model of NAFLD and later challenged these animals with a moderate dose of lipopolysaccharide (LPS). We demonstrated that endotoxemia exacerbated the hepatic inflammatory response and mortality in HFCD-fed mice. The LPS-activated hepatic NK cells secrete IFN-γ, which induces massive recruitment and polarization of a specific subpopulation of neutrophils expressing PD-L1. This subpopulation of neutrophils releases a high concentration of TNF-α, which mediates the liver lesion and increases the mortality of the animals. Biological treatments promoting PD-L1 neutralization, or neutrophil depletion, reduced the TNFα concentration and improved the liver inflammatory response, organ pathology, and survival in endotoxemic HFCD-fed mice. Similar results were observed with the use of genetic knockout TNF-α receptor mice. Thus, our findings describe the potential mechanism involved in the exacerbation of neutrophil activity in NAFLD mice and suggest biological interventions as a viable pharmacological approach to abolish the hyper-inflammatory response observed in pathological hepatic conditions

2. RESULTS

NAFLD mice are more susceptible to LPS-induced systemic inflammation.

To study NAFLD as a pre-condition associated with increasing risk of exacerbation of inflammation induced by endotoxemia, we employed a murine model NAFLD in which the mice were fed for two weeks with a choline-deficient high-fat HFCD diet, a well-known liver disease model (Fig 1A). The protocol was modified due to the observation that lymphocytes decreased in number over the weeks of the eight-week HFCD diet. As a result, we used a two-week diet period during which no changes in lymphocyte numbers were observed because the HFCD diet, which is choline-deficient, leads to a reduction in lymphocyte numbers in the animals (20). The HFCD mice challenged with LPS (10 mg/kg; intraperitoneally triggered an elevated susceptibility with an index of mortality of 100% 24 h after the challenge (Fig 1B). In our experimental condition, this dose of LPS provoked moderate (below 40%, 4 days after LPS challenge) mortality in chow-fed mice (control group), (Fig 1B). Compared with the control group the HFCD animals challenged with LPS showed elevated liver damage evidenced by an increase of plasmatic alanine aminotransferase (ALT) levels (a known marker of liver injury) and histopathological alteration, characterized by leukocyte infiltration and edema (Fig 1C,1E). Compared with control mice treated with PBS, the HFCD animals also treated with PBS did not show significative signs of hepatic damage and local inflammatory response, evidenced by the absence of leukocyte infiltration (Fig1C and 1E). Remarkably, compared with the Chow group, HFCD mice exposed to LPS did not exhibit higher kidney injuries (Figure 1D), indicating a pathological inflammatory condition is increased mainly in liver tissue compared to other organs. To assess how NAFLD modulates the immune response in the hepatic microenvironment of human patients, we reanalyzed previously published bulk RNA-seq data from patients with NAFLD to identify potential targets related to the inflammatory process(21). Firstly, we performed analyses of genes differentially expressed in leukocyte samples from patients with NAFLD and healthy controls. We observed that 5240 genes are upregulated, such as *EIF4H*, *TMEM*, *MOB1A*, *SERBP1*, *TM9SF1*, *HINT3*, *ARF3*, *CHTF8*, and *PDIA6*, while 5806 genes, as *FOSB*, *KAT2A*, *SNRNP70*, *CCNL2*, *AMY2B*, *EXD3*, and *EBNA1BP2, are* downregulated. Interestingly, the *CD274* gene (encoding PD-L1) and the *IFNGR2* gene, corresponding to the IFN-γ receptor, are among the upregulated genes (Fig2A).

Furthermore, after conducting an additional enrichment analysis of the 5240 upregulated genes using Gene Ontology (GO), we detected an increase in several pathways associated with an inflammatory process, such as phagocytosis, leukocyte migration, immune response to bacterial components, and IL1β, TNFα, and IFN-γ-referred signaling (Fig2B).

Because IFN-γ and TNF-α signaling pathways are upregulated in NAFLD patients, we reanalyzed previously published single-cell RNA-seq data from liver samples from mice fed with a 60% high-fat diet, another known NAFLD model(22). We noted an increase in immune cells in the hepatic tissue, such as monocytes, neutrophils, dendritic cells, T cells, and NK cells (Fig 2C and 2D). Interestingly, we observed a specific upregulation of CD274 and TNFα genes in monocytes and neutrophils, while T cells and NK cells showed increased IFN-γ expression in T and NK cells (Fig 2E), suggesting that the cytokines produced by these specific cells may be involved in the hyperinflammation observed during NAFLD.

Next, based on the results of increased IFN-γ and TNF-α signaling in bulk RNAseq and single-cell RNA sequencing analyses in hepatic samples of NAFLD patients and animals, we investigated the role of these cytokines in the susceptibility of endotoxemic NAFLD mice. Initially, we observed an exacerbated hepatic production of both cytokines induced by endotoxin challenge in the HFCD-fed group compared to the control mice treated with PBS or LPS (Fig3A and 3B). Furthermore, we also observed that IFN-$\gamma^{-/-}$ and TNFR1R2$\alpha^{-/-}$ mice with NAFLD challenged with LPS did not show an increase of the enzyme ALT, a liver lesions marker (Fig3C and 3D). In addition, endotoxemic NAFLD TNFR1R2$^{-/-}$ and IFN-$\gamma^{-/-}$ mice exhibited reduced leukocyte infiltration in the liver tissue and improved survival (Fig3E, 3F, and 3G), respectively, as compared to endotoxemic WT mice. Together, our data demonstrate that NAFLD predisposes to the exacerbation of cytokines production, such as IFN-γ and TNF, which mediate an elevated mortality index in endotoxemic mice.

NAFLD induces the recruitment of NK cells that are sources of IFN-γ production in endotoxemia

During the inflammatory process, it is already established that CD4 and CD8 T cells are important sources of IFN-γ(23). Herein, we observed a selective increase in IFN-γ production by CD8, but not CD4, T cells (Fig 4A, Fig4B, S1B, S1A), respectively. In light of this, we next investigated the involvement of lymphoid cells in the high

susceptibility of endotoxemic mice with NAFLD. For this, we submitted animals with the absence of T and B cells (*Rag1*$^{-/-}$ mice) to NAFLD protocol. After challenging them with LPS,the survival rate was assessed. Interestingly, *Rag1*-deficient animals under the HFCD diet remained susceptible to the LPS challenge (Fig 4C), suggesting that these T and B cells do not contribute to susceptibility to the LPS challenge.

Recent studies have demonstrated that NK cells are other IFN-γ-producing cells recruited to the hepatic tissue during NAFLD and that they are also involved in systemic inflammatory responses, including sepsis(24–29). We observed that the number of NK cells is increased in the hepatic tissue of NAFLD animals, compared with mice fed with a control chow diet. The challenge with LPS enhanced the NK accumulation in liver tissue only in NAFLD mice (FigS1C and 4D). Furthermore, our cytometric analyses demonstrated that NK cells infiltrated in the liver tissue secrete high levels of IFN-γ (FigS1D and 4E). Next, to confirm the pathological involvement of NK cells during hyperinflammation in NAFLD, we depleted these cells by treating animals with anti-NK antibody 1.1, one day before the LPS challenge (FigS2). Interestingly, the pharmacological depletion of NK cells in NAFLD animals provoked an increased survival index (Fig4F). Furthermore, when NK cells were depleted, NAFLD animals exhibited reduced hepatic damage (Fig4G), IFN-γ levels (Fig4H), and TNFα levels (Fig4I). Together, these results suggest that NK cells are responsible for an increase in the mortality via IFN-γ production in NAFLD during endotoxemia.

Neutrophils are responsible for susceptibility during hyperinflammation in NAFLD

During NAFLD development, innate immune cells, such as monocytes and neutrophils, are the first leukocytes recruited to the liver (24, 30). With this in mind, mice with NAFLD were challenged with LPS, and the infiltration of these cells in the liver was quantified. During the initial inflammatory phase, six hours after the LPS challenge, we observed that monocytes were recruited to the site (Fig5A and 5B). Since inflammatory monocytes emigrate from the bone marrow towards the periphery via CCR2 and then migrate to inflamed tissues, differentiating into monocytes-derived macrophages (30, 31), we investigated the functional role of monocytes in NAFLD, using CCR2-deficient mice (Fig3S). Interestingly, animals deficient in monocyte migration (CCR2-/-) showed a high mortality rate, compared with wild type after LPS challenge (Fig3SA and 3SB). Furthermore, the survival rate of NAFLD CCR2-/- mice

challenged with LPS was not different of NAFLD wild-type mice also challenged with LPS (Fig 3SB). Together, the results suggest that monocytes do not contribute to susceptibility in endotoxemic animals with NAFLD

In addition to monocytes, granulocytes are innate immune cells recruited to the hepatic tissue during the development of NAFLD(19). We observed that high levels of neutrophils are present in the hepatic tissue of animals with NAFLD and that their recruitment is exacerbated in the hepatic microenvironment in endotoxemic mice (Fig5A and 5C). It is known that neutrophils are recruited to the inflammatory focus via CXCR2(32). To understand the involvement of these receptors and neutrophils in NAFLD during endotoxemia, NAFLD animals were pre-treated one day before the LPS challenge with CXCR2i or with anti-Ly6G, which depletes these cells throughout the organism. Interestingly, after both treatments, we observed a reduction of the leukocyte infiltration into the hepatic tissue (Fig5D) and a decrease in hepatic lesions (ALT) (Fig5E) and TNFα levels (Fig5F). Confirming the participation of granulocytes in susceptibility after the LPS challenge in NAFLD, animals treated with CXCR2i and anti-Ly6G showed an improvement in their survival (Fig5G and 5H).

IFN-γ induces CD274 expression during endotoxemia in animals with NAFLD

IFN-γ is a cytokine that plays a crucial role in the T and NK cell-mediated immune response(27–29, 33–35). Recent studies have shown that this inflammatory cytokine also induces the expression of checkpoint molecules, such as programmed death-ligand 1 (PD-L1) in different immune cells, including neutrophils(30, 36, 37). Analyzing datasets from mice with NAFLD, we observed the upregulation of the CD274 (PD-L1) gene and TNF-α in neutrophils and IFN-γ in NK cells (Fig1C, Fig1D, and Fig1E). Considering these findings, we investigated whether IFN-γ induces the expression of PD-L1 in neutrophils in NAFLD mice during endotoxemia. First, we observed that only the NAFLD diet provoked a significant increase in the PD-L1 expression in the hepatic neutrophils (Fig6A). When challenged with LPS, these HFCD-fed mice show an exacerbated migration of PD-L1+ neutrophils toward the liver (Fig6B). Next, to confirm the role of IFN-γ in the expression of PD-L1, we investigated whether IFN-γ enhances the expression of PD-L1 in neutrophils after the LPS challenge of NAFLD. Mice with NAFLD lacking IFN-γ were challenged with LPS and assessed for PD-L1 expression in granulocytes. Interestingly, in the absence of IFN-

γ, neutrophils do not express PD-L1, and their infiltration in the liver was attenuated (Fig6C and 6D).

As demonstrated previously in sepsis, PD-L1 neutrophils showed reduced rates of apoptosis(36). Therefore, we cultured neutrophils in the presence of IFN-γ and LPS and assessed their apoptosis rate. Interestingly, in these *in vitro* conditions, neutrophils expressing PD-L1 showed reduced rates of apoptosis (Fig6E and 6F), suggesting that PD-L1-expressing neutrophils can survive for long periods in the hepatic environment in NAFLD accentuating the LPS-induced inflammatory response.

Neutrophils expressing PD-L1+ secrete TNFα during hyperinflammation in NAFLD

There is also evidence that excessive secretion of TNF-α by immune cells, especially neutrophils, may be associated with liver damage and the progression of NAFLD(36, 37). To investigate a possible link between the expression of PD-L1 by the neutrophils and their ability to express TNF-α, mice undergoing NAFLD were exposed to LPS, and the expression of TNF-α by PD-L1+ neutrophils was assessed. We observed an exacerbated TNF-α expression by PD-L1+ neutrophils from NAFLD compared to control chow animals (Fig7A, Fig7B, and Fig7D). These results illustrate that after exposure of NAFLD animals with LPS, the expression of PD-L1 by neutrophils is linked to heightened TNF-α expression compared to control animals fed standard chow. To assess whether the lack of TNFα signaling immunomodulates the granulocytic recruitment to the liver tissues in NAFLD animals, TNF receptor R1 and R2 knockout animals (TNF R1R2) were exposed to LPS. It was also observed that the absence of TNFα did not interfere with the recruitment of neutrophils to the liver tissue (FigS5A and FigS5C) or the expression of PD-L1 in neutrophils (FigS5B and FigS5D). Similarly, the absence of TNF-α receptors in NAFLD during the challenge with LPS did not interfere with the production of IL-10 and IFN-γ (FigS5E and FigS5G). However, as described above, the absence of the TNF R1R2 receptor reduced liver injury and the mortality induced by LPS administration in NAFLD (Fig3D and Fig 3F).

Considering that NK cells in the liver tissue secrete IFN-γ (Fig 4E), we next examined whether PD-L1+TNFα+ neutrophils are present in NAFLD animals depleted of NK cells. It was observed that in the absence of NK cells, PD-L1+TNFα+ neutrophils were not detected (Fig7E, Fig7F, and Fig7G), confirming that IFN-γ secreted by NK

cells is crucial for inducing PD-L1 expression and TNFα secretion by neutrophils in the hepatic tissue in NAFLD animals after LPS administration.

Anti-PD-L1 treatment protects animals with NAFLD during hyperinflammation

Next, we investigated the potential role of PD-L1 in TNF-α production by neutrophils and in the lesions in NAFLD mice. We found that anti-PD-L1, a biological drug inhibiting PD-L1's interaction with PD-1, effectively prevented liver inflammation and tissue damage (Fig 8A, Fig8B, and Fig8F). Additionally, this treatment reduced liver TNFα levels without affecting IFN-γ (Fig8C) and improved host survival (Figure 8D). Importantly, anti-PD-L1 did not decrease the number of recruited NK cells in all groups studied (Fig8I and Fig8L). Notably, treatment with anti-PD-L1 successfully blocked LPS-induced neutrophil recruitment and the increased presence of PD-L1-expressing neutrophils in mice on HFCD (Fig8J and Fig8L). On the other hand, these parameters remained unchanged in mice fed a standard chow diet (Fig8G, Fig8H). Overall, our findings suggest that anti-PD-L1 therapy decreased neutrophil-derived TNFα production in NAFLD mice without affecting the IFN-γ secretory activity of NK cells.

3. DISCUSSION

The pathogenesis of NAFLD and sepsis had been considered two independent conditions, associated with local and systemic inflammatory response, respectively. NAFLD is a chronic liver dysfunction characterized by the buildup of fat in the liver in individuals who do not consume excessive amounts of alcohol. On the other hand, sepsis is an inflammatory state triggered by an infection that damage vital organs, including the lungs and liver. This hyper-inflammatory response occurs when the body's immune response fails to contain the microorganisms at the site of the primary infection(9). Recent studies demonstrate that the presence of NAFLD is associated with an increased risk of developing sepsis(38, 39), but the exact mechanisms underlying this association are not fully understood. In the present study, we observed that NAFLD mice induced by an HFDC diet are more susceptible to a systemic and hepatic hyper-inflammatory state induced by endotoxemia, confirming in our experimental condition that NAFLD can be considered a crucial risk factor of sepsis progression, even when NAFLD or hepatic inflammation is not yet detected. After, we used this model to explore the cellular and molecular mechanisms involved in the increased susceptibility induced by endotoxemia in NAFLD animals. The LPS administration promotes the polarization of a specific subset of granulocytes expressing PD-L1, which secrete high levels of TNF-α in an NK-derived IFN-γ dependent manner. The released TNF-α plays an important role in the liver lesion. We also observed that CD4+ and CD8+ T cells or monocyte cells do not participate in the mice’s susceptibility during this hyper-inflammatory state. In accordance, previous studies implied NK cells in liver injuries in different NAFLD and sepsis experimental models(25, 40–44). It was observed that during severe sepsis, NK cells and NK cells-released IFN-γ play a detrimental role in mediating tissue injury (44). Similarly, in NAFLD, NK cells can accumulate in the liver and release IFN-γ, which contributes to the development of hepatic inflammation and fibrosis(45). These studies, together with our results, support that the increase in NK cells in endotoxemic NAFLD animals, along with IFN-γ secretion, contribute to hepatic disease progression.

Considering this evidence, we re-analyzed previously published bioinformatic data(21, 22) and observed that, in NAFLD patients, IFN-γ and TNFα are up-regulated, and that, in high-fat high fructose diet-fed mice, there is up-regulation of IFN-γ in NK cells, and TNFα and CD274 (PD-L1) in myeloid cells(21, 22), suggesting that similar immune dysfunctions are observed in patients and experimental model of NAFLD. To

add experimental information about how the IFN-γ mediates the liver lesion, we demonstrated that, in endotoxemic NAFLD animals, hepatic neutrophils are important producers of TNFα, and this release is stimulated by NK-derived IFN-γ signaling. In addition, IFN-γ promoted the differentiation of PDL-1 expressing neutrophils, given that in those animals depleted of NK, the neutrophils did not exhibit this activated phenotype. Moreover, the PDL-1-expressing neutrophils showed a reduced apoptosis rate, increasing the retention time of the neutrophils in hepatic tissue. Thus, these events could explain the increase in hepatic injury in NAFLD animals during endotoxemia. According, to the context of infection-triggered inflammation, the participation of IFN-γ in the modulation of neutrophil pro-inflammatory profiles, including the expression of PD-L1, has been demonstrated (36). Neutrophils, as frontline innate immune cells, control pathogens through phagocytosis and the release of microbial mediators, including cytokines, cytosolic enzymes, free radicals, and NETs (46, 47). However, excessive neutrophil activity can lead to tissue damagewhere they contribute significantly to multi-organ damage via the overproduction of inflammatory mediators, including TNF-α(16, 48, 49). During NAFLD, liver neutrophils are major sources of TNF-α production induced by endotoxemia. Confirming the involvement of TNF-α release by PDL-1+ neutrophils stimulated by NK cells-derived IFN-γ in the increase of susceptibility of NAFLD, we demonstrated that the absence of TNF-α signaling or depleted NK cells led to improved survival in mice with NAFLD during endotoxemia. However, the deficiency of TNF-α signaling did not affect PD-L1 expression in neutrophils. These findings imply that, while TNFα plays a crucial tissue lesion role, its intracellular signaling does not impair the expression of PD-L1 in the neutrophils or their migration into liver tissue during NAFLD. To reinforce that neutrophils are the main source of the TNFα involved in susceptibility of NAFLD by endotoxemia, we evaluate whether neutralizing these cells with specific antibodies could improve the survival of endotoxemic HFDC-fed mice. Numerous strategies targeting neutrophils have been investigated in clinical and experimental settings (12, 50) including the use of CXCR2 inhibitors in NASH patients(13, 50). Interestingly, we demonstrated that targeting neutrophils with different biological drugs, similar to the inhibition of TNF-α, mitigated inflammation-induced liver lesions.

Recent studies suggest that during the progression of NAFLD, PD-L1 is expressed in both parenchymal and non-parenchymal cells(10, 51). Given that the neutrophils responsible for hepatic damage in endotoxemic NAFLD mice exhibit a

specific PD-L1-expressing phenotype, *we* demonstrated that anti-PD-L1 significantly reduced TNFα-producing PD-L1+ neutrophils in the liver environment, attenuating endotoxemia-induced inflammation and liver damage, ultimately reducing mortality in NAFLD mice. This highlights the role of PD-L1 expression in neutrophils in promoting a proinflammatory phenotype associated with heightened TNFα production and susceptibility of endotoxemic HFDC-fed mice. In the context of endotoxemia, recent research indicates that PD-L1-expressing neutrophils also contribute to immunosuppression and increased susceptibility to secondary infections (52) and also contribute to lung injury [36]. Thus, our data support that the PD-L1 inhibition, besides preventing the organ lesions induced by hyper-inflammatory responses in NAFLD patients could also abolish the long-term immunosuppression observed in these patients.

Although macrophages, including Kupffer cells, have been considered a relevant source of cytokines in endotoxemic animals(53, 54), we did not find an important role for these cells expressing CCR2 in the aggravation of endotoxemia, since the absence of this chemokine receptor, which governs the migration and differentiation of monocytes into macrophages, did not influence the endotoxemia mortality in animals with NAFLD. However, it’s worth noting that we did not extensively investigate the interaction of IFN-γ and TNF-α in the role of monocytes in our model, necessitating further studies to unravel the possible mechanisms of these cells.

Overall, our findings establish a biological basis for understanding the progression of endotoxemia in NAFLD, highlighting the dysregulated role of neutrophils in which hepatic metabolic syndrome potentiates the inflammatory effects of granulocytes via NK cells, advocating interventions to mitigate this inflammatory condition.

4. MATERIAL AND METHODS

Experimental Design

This study was designed to interrogate the pathologic mechanisms in NAFLD during endotoxemia-induced generalized inflammation. The mice were submitted to the HFDC diet for two weeks and subsequently, LPS administration and the cellular mechanisms were outlined after 6h of the challenge knowing that no animal succumbs to death (indicated by survival). Inflammatory infiltrates along with liver lesions were assessed based on H&E stained tissue sections and endpoint analyses included flow cytometry.

Animals

The mice used in this study were in the C57BL/6 genetic background and included CCR2 $^{-/-}$, IFN$^{-/-}$, and TNFR1R2 $^{-/-}$. Male mice aged 5 to 6 weeks were reared and maintained under specific pathogen-free conditions in the University of São Paulo vivarium, FMRP/USP. All animals received food and water ad libitum, at 25 °C, with food and water ad libitum. Mice were fed a standard low-fat diet (hereinafter referred to as the standard “Chow” diet – 10% of calories derived from fat) or a high-fat, choline-deficient diet (referred to as “HFCD” 60% of calories derived from fat and choline-deficient) for 2 weeks for the development of NAFLD. The diets were provided by Rhoster (Araçoiaba da Serra- São Paulo). Care for the mice complied with institutional guidelines on ethics in animal experiments; approved by CETEA (Ethics Committee for Animal Experimentation of the Faculty of Medicine of Ribeirão Preto, approved protocol number 193/2019).

Endotoxemia

Lipopolysaccharide (LPS; Escherichia coli (O111:B4), L2630, Sigma-Aldrich, St. Louis, MO, USA) was administrated intraperitoneally (i.p.; 10 mg/kg) in C57BL/6J, CCR2 -/-, IFN$^{-/-}$, TNFR1R2 -/- mice (5 to 6 weeks old, 22 to 26 g body weight). LPS was previously solubilized in sterile saline and frozen at -70ºC freezer. The animals were euthanized 6 hours after LPS administration.

Hepatic non-parenchymal cell isolation

Livers were collected and 200-300 mg of tissue were taken for flow cytometry analysis. The tissue was minced with surgical scissors and then digested with 1 mg of

collagenase II, and 60 U/ml of DNase I in PBS at 37oC for 45 minutes, shaking at 110 rpm. The digested tissue was then processed through a 100 µm cell strainer, and centrifuged at 1,500 rpm for 5 minutes. Subsequently, the isolation of non-parenchymal cells was performed by Percoll (GE Healthcare) centrifuged at 2300rpm at 22oC for 30m, subjected to ACK (red blood cell lysis), and resuspended in 0.5% BSA in PBS for staining. Single-cell suspensions were stained with Zombie Aqua viability stain (Biolegend), blocked with TruStain FcX (Biolegend), and then stained with flow cytometry antibodies when indicated; antibodies are tabulated in Table S1. Cells were collected on the CANTO II flow cytometer using BD FACS Diva software and then analyzed using FlowJo (USA).

Histology

Mouse livers were fixed in 10% formalin overnight, washed twice with PBS, and placed in 70% ethanol or PBS until processing. For H&E, tissues were embedded in paraffin, sectioned, and stained with H&E at the MGH Histopathology Research Core.

Cytokine quantification

For the detection of IFN-γ, TNF-α, and IL-10 in the liver, tissue samples were weighed and titrated in 1 mL of PBS Complete (Roche Diagnostics, Mannheim, Germany) containing a cocktail of protease inhibitors. Cytokine levels were determined using commercial ELISA kits for IFN-γ, TNF-α, and IL-10 (Biolegend, USA). Wavelength correction and background signals were subtracted from absorbance values

Serum analysis

At the time of sacrifice, blood samples were collected in EDTA collection tubes and subsequently centrifuged to obtain serum. Serum ALT and Urea levels were measured using a colorimetric kit (BioQuant, Heidelberg, Germany) according to the manufacturer's instructions.

Neutrophil targeting

For neutrophil targeting, antibodies/inhibitors were used as follows: Anti-Ly6G (BioXCell, catalog # BP0075) was administered at 500 mg/kg per mouse on day 13 after starting the diet (24h before inoculation of the LPS) and sacrificed on day 14. For

survival studies, all mAbs were inoculated once daily for 7 days. CXCR2 inhibitor SB 225002 (Tocris, catalog #2725/10) was injected at 200 mg per dose and programmed as anti-Ly6G. For anti–PD-L1 based neutrophil targeting, anti–PD-L1 (BioXCell, catalog #BE0101) was injected at 12.5 mg/kg ~12h before the LPS challenge and again 1 day after treatment, each time followed by anti-mouse IgG2b (12.5 mg/kg) (BioXCell, catalog no. BE0252). All injections were intraperitoneal.

Neutrophil purification and apoptosis assay

Peripheral blood samples were collected by venipuncture and centrifuged at 450 × g for plasma separation. The blood cells were then resuspended in Hank's balanced salt solution (Corning; cat. 21-022-CV), and the neutrophil population was isolated by Percoll density gradient (GE Healthcare; cat. 17-5445-01) (72 %, 63%, 54% and 45%). Isolated neutrophils were resuspended in RPMI1640 (Corning; cat. 15-040-CVR) supplemented with 0.5% BSA. Neutrophil purity > 95% was determined by Rosenfeld color Cytospin (Laborclin; cat.620529)

To quantify apoptosis, cells were permeabilized with Triton X-100 and stained with propidium iodide. After 10 minutes of incubation at 4 degrees in the dark, neutrophil apoptosis was quantified as PI+ staining on FACSCanto II (Becton Dickinson, Franklin Lakes, NJ, USA). Results were analyzed using Flowjo software (Tree Star, Ashland, OR, USA). Apoptosis was detected as a measure of the hypodiploid peak in PI fluorescence histograms, as described by Nicoletti et al. BD Bioscience, Franklin Lakes, NJ, USA) and Annexin V and 7-AAD double staining (Biolegend, San Diego, USA).

NK cell depletion

For in vivo NK cell depletion, male C57BL/6 mice received NK cell neutralizing antibody (BioXCell, catalog # PK136) or isotype-matched mouse IgG2α monoclonal antibody control (BioXCell, catalog # BE0252) by intraperitoneal injection (150 μg in 200 μL PBS 24h before LPS challenge). To assess survival, it was inoculated 24 hours before the LPS challenge and then once a day for 7 days.

Single-cell RNA sequencing analysis

We re-analyzed single-cell transcriptomic data (GSE166504) from mouse liver from mice with NAFLD and their respective control groups (21). The dataset was

downloaded and the RDS file was imported into R(55) environment version v4.2.3 and Seurat v4.1.1(56) by filtering genes expressed in at least 300 cells. For the pre-processing step, outlier cells were filtered out based on three metrics (library size < 20,000, number of expressed genes between 200 and 4,000, and mitochondrial percentage expression < 0,8). The top 3,000 variable genes were then identified using the 'best' method using the FindVariableFeatures function. Percent of mitochondrial genes was regressed out in the scaling step, and Principal Component Analysis (PCA) was performed using the top 3,000 variable genes and the top 30 PCs were selected for dimension reduction by Uniform Manifold Approximation and Projection (UMAP). Clusters were identified using the author's annotation. Then, differential gene expression analysis was performed using the FindAllMarkers function in Seurat with default parameters to obtain a list of significant gene markers for each cluster of cells. Visualization of genes illustrating expression levels was performed using R/Seurat commands (DimPlot, FeaturePlot, and DotPlot) using ggplot2(57) and customized (58) R packages.

RNA sequencing analysis

RNA-seq data were obtained from GSE185051 (59). The R/Bioconductor package edgeR was used to identify differentially expressed genes among the samples, after removing absent features (zero counts in more than 75% of samples) (60). Genes with a fold change of >0.5 were identified as differentially expressed.

Pathway enrichment analysis

The list of differentially expressed genes was enriched using the ClusterProfiler R package (8). Gene ontology (GO) terms in the Biological Processes category with $P < 0.05$ were considered significant. Statistically significant, non-redundant GO-enriched terms were plotted.

Statistics

Statistical significance was determined by two-tailed paired or unpaired Student's t-test or one-way ANOVA followed by Tukey's post hoc test. Absolute numbers and percentages were compared using Fisher's exact test. Spearman rank order correlation (r) was calculated to describe the correlations. $P<0.05$ was

considered statistically significant. Statistical analyses and graphics were performed using the GraphPad Prism 8.4.2 software.

Author contributions: CCOB, AK, and FQC designed the study. CCOB, AK, and GCMC performed the mouse experiments. CCOB, AK, and FQC wrote the manuscript. GVLS performed the analysis bioinformatic. CCOB, AK, GVLS, GCMC, LOL, TMC, JCFAF, and FQC reviewed the manuscript.

Competing interests

The authors declare no competing interests.

Funding

Funding The research received funding from S~ ao Paulo Research Foundation (FAPESP, 2009/54014-7, 2011/19670, 2012/10438-0 and 2013/08216-2, Center for Research in Inflammatory Diseases), Coodernação de Aperfeiçoamento de Pessoal de Nivel Superior (CAPES) and Conselho Nacional de Desenvolvimento Científico e Tecnológico (CNPq)

Acknowledgements

We thank members of Group FQC for their advice and clinical assistance; and Marcella, Sergio R. Rosa, Katia Santos, Ieda Schivo for technical assistance.

References

1. Younossi ZM, et al. Global epidemiology of nonalcoholic fatty liver disease—Meta-analytic assessment of prevalence, incidence, and outcomes. *Hepatology*. 2016;64(1):73–84.

2. Younossi Z, et al. Global burden of NAFLD and NASH: trends, predictions, risk factors and prevention. *Nature Reviews Gastroenterology & Hepatology 2017 15:1*. 2017;15(1):11–20.

3. Paik JM, et al. Changes in the Global Burden of Chronic Liver Diseases From 2012 to 2017: The Growing Impact of NAFLD. *Hepatology*. 2020;72(5):1605–1616.

4. Estes C, et al. Modeling the epidemic of nonalcoholic fatty liver disease demonstrates an exponential increase in burden of disease. *Hepatology*. 2018;67(1):123–133.

5. Wong RJ, Cheung R, Ahmed A. Nonalcoholic Steatohepatitis Is the Most Rapidly Growing Indication for Liver Transplantation in Patients With Hepatocellular Carcinoma in the U.S. [published online ahead of print: 2014]. https://doi.org/10.1002/hep.26986.

6. Schuster S, et al. Triggering and resolution of inflammation in NASH [preprint]. *Nat Rev Gastroenterol Hepatol*. 2018;15(6):349–364.

7. Peiseler M, Tacke F. Inflammatory Mechanisms Underlying Nonalcoholic Steatohepatitis and the Transition to Hepatocellular Carcinoma. *Cancers (Basel)*. 2021;13(4):1–26.

8. Carpino G, et al. Increased Liver Localization of Lipopolysaccharides in Human and Experimental NAFLD. *Hepatology*. 2020;72(2):470–485.

9. Ferro D, et al. New Insights into the Pathogenesis of Non-Alcoholic Fatty Liver Disease: Gut-Derived Lipopolysaccharides and Oxidative Stress. [published online ahead of print: 2020]. https://doi.org/10.3390/nu12092762.

10. Lombardi R, et al. PD-1/PD-L1 Immuno-Mediated Therapy in NAFLD: Advantages and Obstacles in the Treatment of Advanced Disease. *Int J Mol Sci*. 2022;23(5). https://doi.org/10.3390/IJMS23052707.

11. Smith SR, et al. The cooperative effects of TNF-alpha and IFN-gamma are determining factors in the ability of IL-10 to protect mice from lethal endotoxemia. *J Leukoc Biol*. 1994;55(6):711–718.

12. Abe T, et al. Epidemiology of sepsis and septic shock in intensive care units between sepsis-2 and sepsis-3 populations: sepsis prognostication in intensive care unit and emergency room (SPICE-ICU). *J Intensive Care*. 2020;8(1):1–9.

13. Sakr Y, et al. Open Forum Infectious Diseases Open Forum Infectious Diseases ® Sepsis in Intensive Care Unit Patients: Worldwide Data From the Intensive Care over Nations Audit. https://doi.org/10.1093/ofid/ofy313.

14. Mcdonald B, Kubes P. Neutrophils and intravascular immunity in the liver during infection and sterile inflammation. *Toxicol Pathol*. 2012;40(2):157–165.

15. Jenne CN, Kubes P. Immune surveillance by the liver. *Nat Immunol*. 2013;14(10):996–1006.

16. Michels EHA, et al. Association between age and the host response in critically ill patients with sepsis. *Crit Care*. 2022;26(1). https://doi.org/10.1186/S13054-022-04266-9/FIGURES/5.

17. Bouza C, López-Cuadrado T. Epidemiology and Trends of Sepsis in Young Adults Aged 20-44 Years: A Nationwide Population-Based Study. *J Clin Med*. 2019;9(1). https://doi.org/10.3390/JCM9010077.

18. Knoop ST, et al. Epidemiology and impact on all-cause mortality of sepsis in Norwegian hospitals: A national retrospective study. *PLoS One*. 2017;12(11). https://doi.org/10.1371/JOURNAL.PONE.0187990.

19. Ebrahimi F, et al. Risk of Severe Infection in Patients With Biopsy-proven Nonalcoholic Fatty Liver Disease – A Population-based Cohort Study. *Clinical Gastroenterology and Hepatology*. 2023;21(13):3346-3355.e19.

20. Raubenheimer PJ, Nyirenda MJ, Walker BR. A Choline-Deficient Diet Exacerbates Fatty Liver but Attenuates Insulin Resistance and Glucose Intolerance in Mice Fed a High-Fat Diet. *Diabetes*. 2006;55(7):2015–2020.

21. Yao K, et al. Transcriptomic profiling of a multiethnic pediatric NAFLD cohort reveals genes and pathways associated with disease. *Hepatol Commun*. 2022;6(7):1598–1610.

22. Su Q, et al. Single-cell RNA transcriptome landscape of hepatocytes and non-parenchymal cells in healthy and NAFLD mouse liver. *iScience*. 2021;24(11). https://doi.org/10.1016/J.ISCI.2021.103233.

23. Burke JD, Young HA. IFN-γ: A cytokine at the right time, is in the right place. *Semin Immunol*. 2019;43. https://doi.org/10.1016/J.SMIM.2019.05.002.

24. Amer J, et al. Insulin signaling as a potential natural killer cell checkpoint in fatty liver disease. *Hepatol Commun*. 2018;2(3):285–298.

25. Martínez-Chantar ML, Delgado TC, Beraza N. Revisiting the Role of Natural Killer Cells in Non-Alcoholic Fatty Liver Disease. *Front Immunol*. 2021;12:640869.

26. Wang F, et al. Activated Natural Killer Cell Promotes Nonalcoholic Steatohepatitis Through Mediating JAK/STAT Pathway. *Cell Mol Gastroenterol Hepatol*. 2022;13(1):257.

27. He H, et al. NK cells promote neutrophil recruitment in the brain during sepsis-induced neuroinflammation. *Sci Rep*. 2016;6. https://doi.org/10.1038/SREP27711.

28. Jensen IJ, et al. Polymicrobial sepsis influences NK-cell-mediated immunity by diminishing NK-cell-intrinsic receptor-mediated effector responses to viral ligands or infections. *PLoS Pathog*. 2018;14(10). https://doi.org/10.1371/JOURNAL.PPAT.1007405.

29. Kumar V. Natural killer cells in sepsis: Underprivileged innate immune cells. *Eur J Cell Biol*. 2019;98(2–4):81–93.

30. Nati M, Chung K-J, Chavakis T. The Role of Innate Immune Cells in Nonalcoholic Fatty Liver Disease Introduction: NAFLD and NASH. [published online ahead of print: 2021]. https://doi.org/10.1159/000518407.

31. Li M, et al. Recent advances targeting C-C chemokine receptor type 2 for liver diseases in monocyte/macrophage. *Liver Int*. 2020;40(12):2928–2936.

32. Metzemaekers M, Gouwy M, Proost P. Neutrophil chemoattractant receptors in health and disease: double-edged swords. *Cellular & Molecular Immunology 2020 17:5*. 2020;17(5):433–450.

33. Eriguchi Y, et al. Essential role of IFN-γ in T cell–associated intestinal inflammation. *JCI Insight*. 2018;3(18). https://doi.org/10.1172/JCI.INSIGHT.121886.

34. Lin Q, et al. IFN-γ-dependent NK cell activation is essential to metastasis suppression by engineered Salmonella. *Nat Commun*. 2021;12(1). https://doi.org/10.1038/S41467-021-22755-3.

35. Arase H, Arase N, Saito T. Interferon gamma production by natural killer (NK) cells and NK1.1+ T cells upon NKR-P1 cross-linking. *J Exp Med*. 1996;183(5):2391–2396.

36. Wang J feng, et al. Upregulated PD-L1 delays human neutrophil apoptosis and promotes lung injury in an experimental mouse model of sepsis. *Blood*. 2021;138(9):806–810.

37. Falcinelli M, et al. Propranolol reduces IFN-γ driven PD-L1 immunosuppression and improves anti-tumour immunity in ovarian cancer. *Brain Behav Immun*. 2023;110:1–12.

38. Acharya C, Bajaj JS. Gut Microbiota and Complications of Liver Disease. *Gastroenterol Clin North Am*. 2017;46(1):155–169.

39. Mohammad S, Thiemermann C. Role of Metabolic Endotoxemia in Systemic Inflammation and Potential Interventions. *Front Immunol*. 2021;11. https://doi.org/10.3389/FIMMU.2020.594150.

40. Chen Y, Tian Z. Roles of Hepatic Innate and Innate-Like Lymphocytes in Nonalcoholic Steatohepatitis. *Front Immunol*. 2020;11. https://doi.org/10.3389/FIMMU.2020.01500.

41. Hwang S, et al. Role of Neutrophils in the Pathogenesis of Nonalcoholic Steatohepatitis. *Front Endocrinol (Lausanne)*. 2021;12. https://doi.org/10.3389/FENDO.2021.751802.

42. Stiglund N, et al. Retained NK Cell Phenotype and Functionality in Non-alcoholic Fatty Liver Disease. *Front Immunol*. 2019;10(JUN). https://doi.org/10.3389/FIMMU.2019.01255.

43. Mantovani A, et al. Neutrophils in the activation and regulation of innate and adaptive immunity. [published online ahead of print: 2011]. https://doi.org/10.1038/nri3024.

44. Zeerleder S, et al. Activated cytotoxic T cells and NK cells in severe sepsis and septic shock and their role in multiple organ dysfunction. *Clin Immunol*. 2005;116(2):158–165.

45. Luo XY, et al. IFN-γ deficiency attenuates hepatic inflammation and fibrosis in a steatohepatitis model induced by a methionine- and choline-deficient high-fat diet. *Am J Physiol Gastrointest Liver Physiol*. 2013;305(12). https://doi.org/10.1152/AJPGI.00193.2013.

46. Rosales C. Neutrophil: A Cell with Many Roles in Inflammation or Several Cell Types? *Front Physiol*. 2018;9(FEB). https://doi.org/10.3389/FPHYS.2018.00113.

47. Kanashiro A, et al. The role of neutrophils in neuro-immune modulation HHS Public Access. https://doi.org/10.1016/j.phrs.2019.104580.

48. Tracey KJ, et al. Shock and tissue injury induced by recombinant human cachectin. *Science*. 1986;234(4775):470–474.

49. Bordon J, et al. Understanding the roles of cytokines and neutrophil activity and neutrophil apoptosis in the protective versus deleterious inflammatory response in pneumonia. *Int J Infect Dis*. 2013;17(2). https://doi.org/10.1016/J.IJID.2012.06.006.

50. Leslie J, et al. CXCR2 inhibition enables NASH-HCC immunotherapy. *Gut*. 2022;71(10):2093–2106.

51. Dong G, et al. Increased PD-L1 Restricts Liver Injury in Nonalcoholic Fatty Liver Disease. *Oxid Med Cell Longev*. 2022;2022. https://doi.org/10.1155/2022/5954437.

52. Thanabalasuriar A, et al. *H E A L T H A N D M E D I C I N E PD-L1 + neutrophils contribute to injury-induced infection susceptibility*. 2021.

53. Huston JM, et al. Splenectomy inactivates the cholinergic antiinflammatory pathway during lethal endotoxemia and polymicrobial sepsis. *J Exp Med*. 2006;203(7):1623–1629.

54. Fonseca MT, et al. A leukotriene-dependent spleen-liver axis drives TNF production in systemic inflammation. *Sci Signal*. 2021;14(679). https://doi.org/10.1126/SCISIGNAL.ABB0969.

55. R: a language and environment for statistical computing [Internet]. https://www.gbif.org/tool/81287/r-a-language-and-environment-for-statistical-computing. Accessed April 18, 2024.

56. Hao Y, et al. Integrated analysis of multimodal single-cell data. *Cell*. 2021;184(13):3573-3587.e29.

57. Wickham H. ggplot2. [published online ahead of print: 2016]. https://doi.org/10.1007/978-3-319-24277-4.

58. scCustomize-package: scCustomize: Custom Visualizations & Functions for... in samuel-marsh/scCustomize: Custom Visualizations & Functions for Streamlined Analyses of Single Cell Sequencing [Internet]. https://rdrr.io/github/samuel-marsh/scCustomize/man/scCustomize-package.html. Accessed April 18, 2024.

59. Chen Y, Lun ATL, Smyth GK. From reads to genes to pathways: Differential expression analysis of RNA-Seq experiments using Rsubread and the edgeR quasi-likelihood pipeline. *F1000Res*. 2016;5. https://doi.org/10.12688/F1000RESEARCH.8987.2/DOI.

60. Wu T, et al. clusterProfiler 4.0: A universal enrichment tool for interpreting omics data. *Innovation (Cambridge (Mass))*. 2021;2(3). https://doi.org/10.1016/J.XINN.2021.100141.

Table S1 Antibodies Cytometry

Anti-mouse CD11b (M1/70) APC-CY7	101226	BioLegend
Anti-mouse CD3 (17A2) FITC	100206	BioLegend
Anti-mouse CD45(30-F11) PE-CY7	103114	BioLegend
Anti-mouse CD8(53-6.7) APC	100712	BioLegend
Anti-mouse IFN-g (XMG1.2) PE	505808	BioLegend
Anti-mouse TNFα PE	506306	BioLegend
Anti-mouse Ly-6G (1A8) FITC	127606	BioLegend
Anti-mouse Ly-6C (HK1.4) PERCP	128028	BioLegend
Anti-mouse MHCII BV510	107636	BioLegend
Anti-mouse NK1.1(PK136) APC-CY7	156510	BioLegend
Anti-mouse PD-L1 APC	124312	BioLegend
Anti-mouse CD4 (GK1.5) PERCP	100432	BioLegend

Figure 1. Mice fed with a high-fat and choline-deficient (HFCD) diet develop non-alcoholic fatty liver disease (NAFLD) and are more susceptible to endotoxemia. (A)

Schematic illustration of the experimental design. (B) Survival curves of mice with NAFLD (n=5) and Chow diet (controls) (n=5) which were injected intraperitoneally with LPS (10mg/kg) and the survival rates were determined daily for 6 days (C and D) Serum ALT and Urea levels from mice with NAFLD and Chow, 6 hours after LPS (10 mg/kg) and PBS administration (n=5). (E) Effect of LPS inoculation on histopathology (H&E stain) of liver from mice with NAFLD or controls (Chow diet). The results are expressed as the mean ± standard deviation (SD) from one representative experiment. Statistical analysis was performed using one-way ANOVA followed by Tukey's multiple comparison test. Statistical significance was determined with the following p-values: *p < 0.05, **p < 0.01, ***p < 0.001. Each experiment was independently repeated 2 times to ensure reproducibility of the findings.

Figure 2. The expression of genes from the inflammatory pathways of IFNγ and TNFα are increased during the development of NAFLD in mice and humans. (A) Volcano plots illustrating the fold change and P-value for gene expression comparisons between livers of NAFLD and healthy patients. Genes of interest are highlighted on the volcano charts. (B) Gene Ontology (GO) functional analysis of differentially expressed genes (DEGs). GO enrichment analysis of DEGs was conducted using DAVID, presenting the 20 most significantly (P < 0.05) enriched GO terms in biological process, molecular function, and cellular component categories. All adjusted statistically significant values are presented as negative log-transformed base 10 values. (C) UMAP plots depicting immune cells from livers of mice subjected to 30 weeks of HFCD diet compared to Chow diet. (D) Frequency distribution of immune cell populations. (E) Expression levels of CD14, CD274, IFNγ, and TNF genes within hepatic immune cell populations.

Figure 3. TNF-α and IFN-γ participate in susceptibility in mice with NAFLD to endotoxemia. (A) IFNγ and (B) TNF-α secretion in the tissue livers of Chow and NAFLD mice injected with LPS (10mg/kg) (n = 5). (C) Serum ALT levels from mice with NAFLD and Chow and/or knockout of IFNγ (IFNγ-/-) and (D) TNFα (TNFR1R2-/-), 6 hours after 10 mg/kg LPS and PBS administration (n=5). (E) Effect of LPS inoculation on liver histopathology from mice with NAFLD and Chow and/or knockout of IFNγ-/- and TNF (TNFR1R2-/-). (F) Survival curves of mice with NAFLD (n=5) and Chow (n=5) and/or knockout of IFN (IFNγ-/-) and (G) TNF (TNFR1R2-/-), after intraperitoneal inoculation of LPS (10mg/kg). The results are expressed as the mean ± standard deviation (SD) from one representative experiment. Statistical analysis was performed using one-way ANOVA followed by Tukey's multiple comparison test. Statistical significance was determined with the following p-values: *p < 0.05, **p < 0.01, ***p < 0.001. Each experiment was independently repeated 2 times to ensure reproducibility of the findings.

Figure 4. IFN-γ secreted by NK cells increases susceptibility of animals with NAFLD to endotoxemia. (A) CD4 IFN+ and (B) CD8 IFN+ T cell frequency in animals

with NAFLD and Chow 6h after LPS inoculation. (C) displays survival curves of mice with NAFLD (n=5) and Chow (n=5) and T-cell knockout (RAg-/-). (D) and (E) represent the number of cells and frequency of NK IFN+ or IFN- in animals with NAFLD and Chow 6h after LPS inoculation (F) The survival curves of mice with NAFLD (n=5) and Chow (n=5) and/or depleted NK cells (Anti NK 1.1), 6 days after intraperitoneal inoculation of LPS (10mg/kg) (G) presents the serum ALT levels from mice with NAFLD and Chow of mice with NAFLD (n=5) and Chow (n=5) and/or depleted NK cells (Anti NK 1.1), 6 hours after 10 mg/kg LPS or PBS administration (n=5). (H) and (I) depict IFN and TNF-α secretion in the livers of Chow and NAFLD mice injected with LPS (10mg/kg) (n=5), respectively. (J) shows TNF-α secretion in the livers of Chow and NAFLD and/or knockout of IFNγ (IFNγ-/-) mice injected with LPS (10mg/kg) (n=5). The results are expressed as the mean ± standard deviation (SD) from one representative experiment. Statistical analysis was performed using one-way ANOVA followed by Tukey's multiple comparison test. Statistical significance was determined with the following p-values: *$p < 0.05$, **$p < 0.01$, ***$p < 0.001$. Each experiment was independently repeated 2 times to ensure reproducibility of the findings.

Figure 5. Neutrophils but not monocytes mediate susceptibility of animals with NAFLD to endotoxemia (A) Representative flow cytometry plot showing monocytes (CD45+CD11b+MHC-Ly6C+Ly6G-) and neutrophils (CD45+CD11b+MHC-Ly6C+Ly6G+) and a number of monocytes (B) and neutrophils (C) in animals with NAFLD and Chow after LPS inoculation. (D) Effect of LPS inoculation on liver histopathology of mice with NAFLD and Chow treated with a CXCR2 inhibitor (CXCR2i) and neutrophil-depleted animals (anti-Ly6G). (E) Serum ALT levels of mice with NAFLD and Chow and/or CXCR2i and anti-Ly6G, 6 hours after administration of 10 mg/kg of LPS and PBS (n=5). (F) TNF-α secretion in the liver of Chow and NAFLD mice injected with LPS (10mg/kg) ($n = 5$). (G) Survival curves of mice with NAFLD (n=5) and Chow (n=5) treated with anti-Ly6G or (H) CXCR2i, and the survival rates were analysed daily for 6 days after intraperitoneal administration of LPS (10mg/kg). The results are expressed as the mean ± standard deviation (SD) from one representative experiment. Statistical analysis was performed using one-way ANOVA followed by Tukey's multiple comparison test. Statistical significance was determined with the following p-values: *$p < 0.05$, **$p < 0.01$, ***$p < 0.001$. Each experiment was independently repeated 2 times to ensure reproducibility of the findings.

Figure 6. IFN-γ induces PD-L1 expression and reduces apoptosis in mouse neutrophils with NAFLD. (A) Representative flow cytometry plot showing the expression of PD-L1 in gated neutrophils and (B) the quantification of PD-L1+ neutrophils in the liver of mice with NAFLD or that received Chow diet, 6 hours after LPS inoculation (n=5 per group). (C) Representative flow cytometry plot showing the expression of PD-L1 in gated neutrophils and (D) the quantification of PD-L1+ neutrophils in the liver of mice with NAFLD and Chow and/or IFNγ knockout (IFNγ-/-) 6 hours after LPS inoculation (n=5 per group). (E) Representative flow cytometry plot showing the expression of PD-L1 and apoptosis (Annexin V+ 7AAD+) in gated neutrophils and (F) the frequency of apoptosis in neutrophils cultured in medium, LPS, IFN, or LPS+IFN for 24 hours. The results are expressed as the mean ± standard deviation (SD) from one representative experiment. Statistical analysis was performed using one-way ANOVA followed by Tukey's multiple comparison test. Statistical significance was determined with the following p-values: *$p < 0.05$, **$p < 0.01$, ***$p < 0.001$. Each experiment was independently repeated 2 times to ensure reproducibility of the findings.

Figure 7. IFN-γ-dependent secretion of TNF-α by PD-L1+ neutrophils induces susceptibility of animals with NAFLD to endotoxemia. (A) Representative flow cytometry plot showing TNF expression in PD-L1+ neutrophils in the liver of animals with NAFLD or fed with Chow diet 6h after LPS inoculation. (B) Number of TNF+ neutrophils. (C) Number of TNF+PD-L1- neutrophils. (D) number of TNF+PD-L1+ neutrophils. (E) Representative flow cytometry plot showing TNF expression in PD-L1+TNF+ neutrophils in the liver of animals with NAFLD and Chow and/or depleted NK cells (anti-NK 1.1) 6h after LPS inoculation. (F) Number of PD-L1+ neutrophils. (G) Frequency of TNF+ neutrophils. The results are expressed as the mean ± standard deviation (SD) from one representative experiment. Statistical analysis was performed using one-way ANOVA followed by Tukey's multiple comparison test. Statistical significance was determined with the following p-values: *$p < 0.05$, **$p < 0.01$, ***$p < 0.001$. Each experiment was independently repeated 2 times to ensure reproducibility of the findings.

Figure 8. Anti PD-L1 treatment reduces PD-L1 neutrophils in animals with NAFLD during endotoxemia. (A) Schematic illustration of experimental design. (B) Serum ALT levels of mice with NAFLD or feded with Chow and/or treated with anti-PDL1, 6 hours after administration of 10 mg/kg of LPS or PBS (n=5). (C) IFN and TNF-α secretion in the liver of Chow and NAFLD mice injected with LPS (10mg/kg) treated with anti-PDL1 (n = 5). (D) Survival curves of mice with NAFLD (n=5) and Chow (n=5) treated or not with anti-PD-L1. (E) Representative flow cytometry graph showing TNF expression in PD-L1+ neutrophils in the liver of animals with NAFLD and Chow and/or treated with anti-PD-L1 6h after LPS inoculation. (F) Effect of LPS inoculation in liver histopathology of mice with NAFLD and Chow treated or not with anti-PD-L1. (G and J) Frequency of PDL1 neutrophils, (H and K) Number of neutrophils, (I and L) Number of NK cells from animals with NAFLD and Chow and/or treated with anti-PDL1 after 6h of LPS inoculation. The results are expressed as the mean ± standard deviation (SD) from one representative experiment. Statistical analysis was performed using one-way ANOVA followed by Tukey's multiple comparison test. Statistical significance was determined with the following p-values: *$p < 0.05$, **$p < 0.01$, ***$p < 0.001$. Each experiment was independently repeated 2 times to ensure reproducibility of the findings.

Figure 1

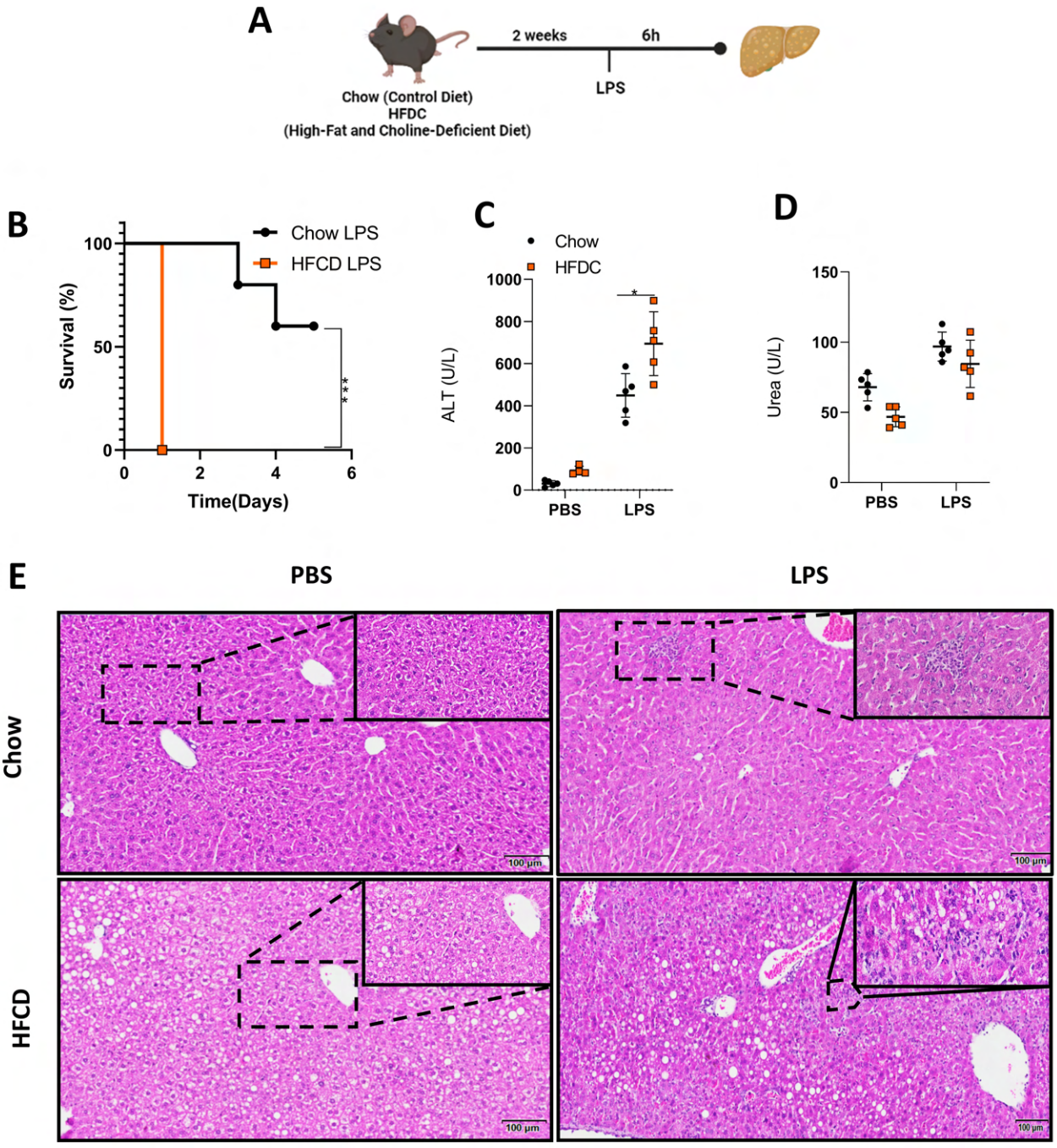
A
2 weeks
6h
LPS
Chow (Control Diet)
HFDC
(High-Fat and Choline-Deficient Diet)
B
Chow LPS
HFCD LPS
Survival (%)
Time(Days)
***
C
Chow
HFDC
ALT (U/L)
PBS
LPS
*
D
Urea (U/L)
PBS
LPS
E
PBS
LPS
Chow
HFCD
100 µm

Figure 2

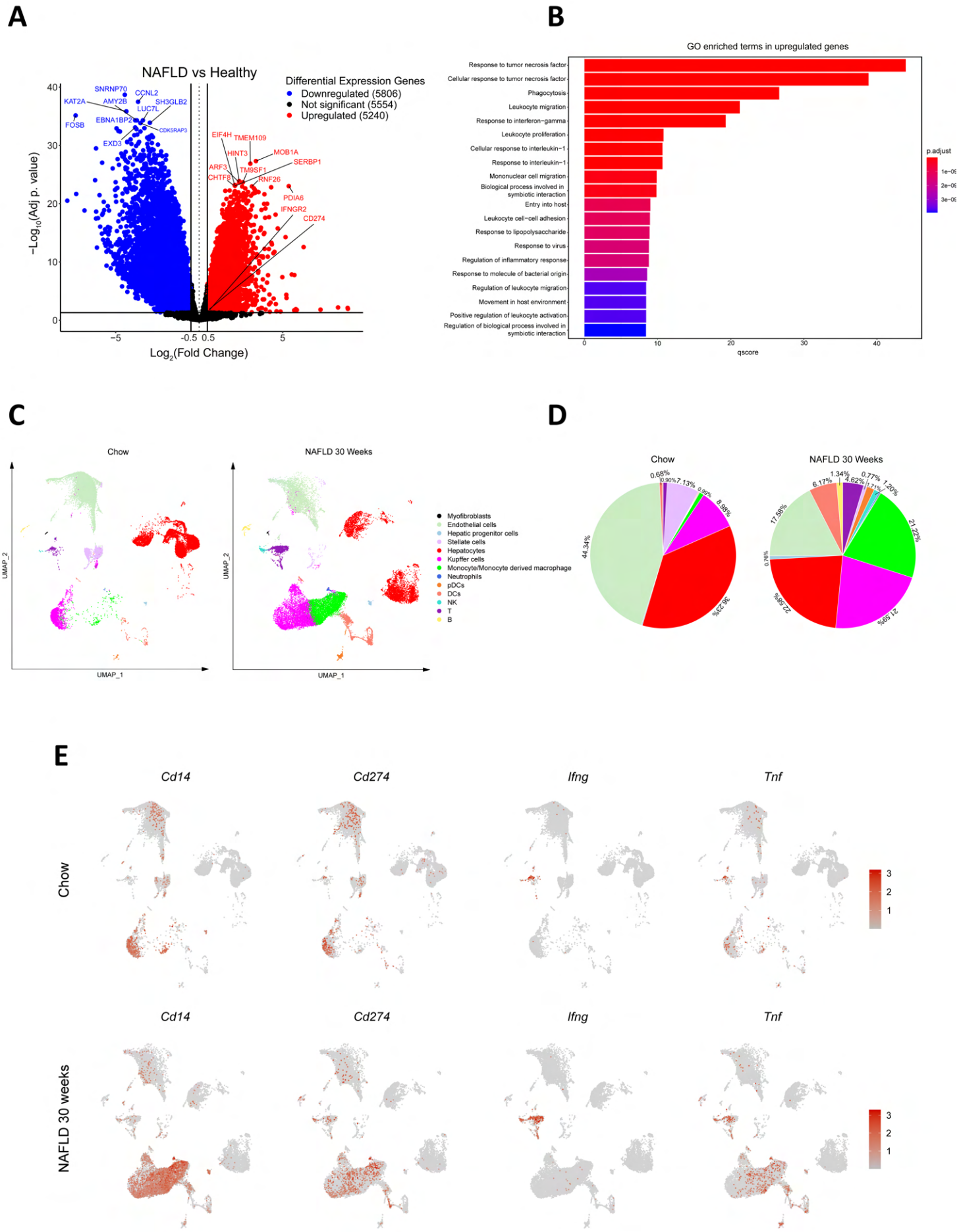
A
NAFLD vs Healthy
Differential Expression Genes
Downregulated (5806)
Not significant (5554)
Upregulated (5240)
SNRNP70
CCNL2
KAT2A
AMY2B
SH3GLB2
LUC7L
FOSB
EBNA1BP2
CDK5RAP3
EXD3
EIF4H
TMEM109
HINT3
MOB1A
SERBP1
ARF3
TM9SF1
CHTF8
RNF26
PDIA6
IFNGR2
CD274
−Log10(Adj p. value)
Log2(Fold Change)
B
GO enriched terms in upregulated genes
Response to tumor necrosis factor
Cellular response to tumor necrosis factor
Phagocytosis
Leukocyte migration
Response to interferon−gamma
Leukocyte proliferation
Cellular response to interleukin−1
Response to interleukin−1
Mononuclear cell migration
Biological process involved in symbiotic interaction
Entry into host
Leukocyte cell−cell adhesion
Response to lipopolysaccharide
Response to virus
Regulation of inflammatory response
Response to molecule of bacterial origin
Regulation of leukocyte migration
Movement in host environment
Positive regulation of leukocyte activation
Regulation of biological process involved in symbiotic interaction
qscore
p.adjust
C
Chow
NAFLD 30 Weeks
UMAP_1
UMAP_2
Myofibroblasts
Endothelial cells
Hepatic progenitor cells
Stellate cells
Hepatocytes
Kupffer cells
Monocyte/Monocyte derived macrophage
Neutrophils
pDCs
DCs
NK
T
B
D
Chow
NAFLD 30 Weeks
E
Cd14
Cd274
Ifng
Tnf
Chow
NAFLD 30 weeks

Figure 3

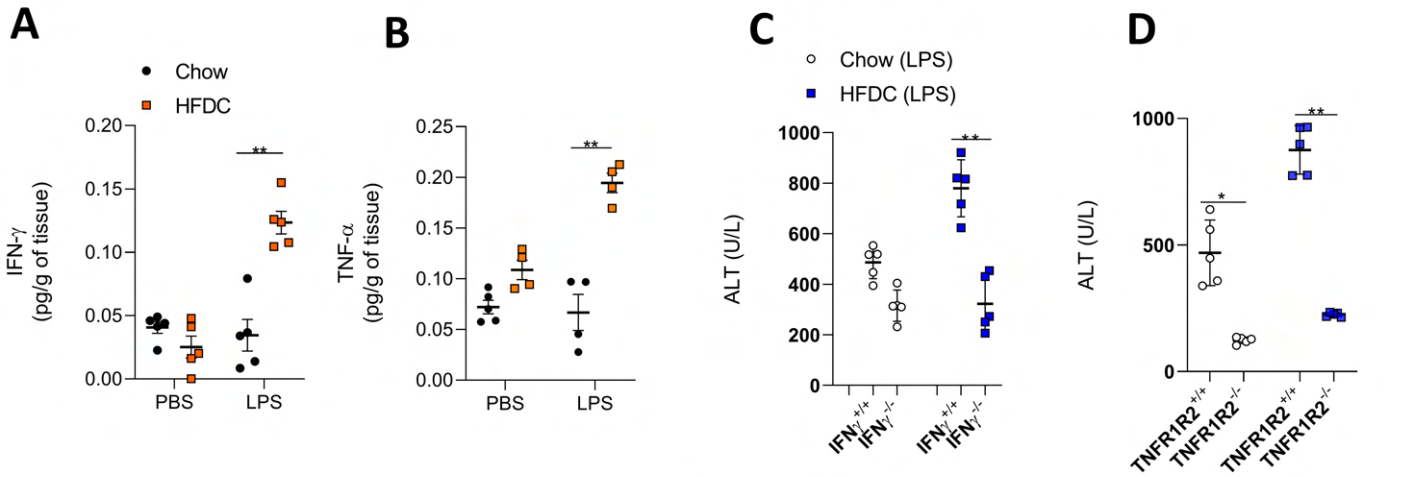
A
Chow
HFDC
IFN-γ (pg/g of tissue)
0.20
0.15
0.10
0.05
0.00
**
PBS
LPS
B
TNF-α (pg/g of tissue)
0.25
0.20
0.15
0.10
0.05
0.00
**
PBS
LPS
C
Chow (LPS)
HFDC (LPS)
ALT (U/L)
1000
800
600
400
200
0
**
IFNγ +/+
IFNγ -/-
IFNγ +/+
IFNγ -/-
D
ALT (U/L)
1000
500
0
*
**
TNFR1R2 +/+
TNFR1R2 -/-
TNFR1R2 +/+
TNFR1R2 -/-

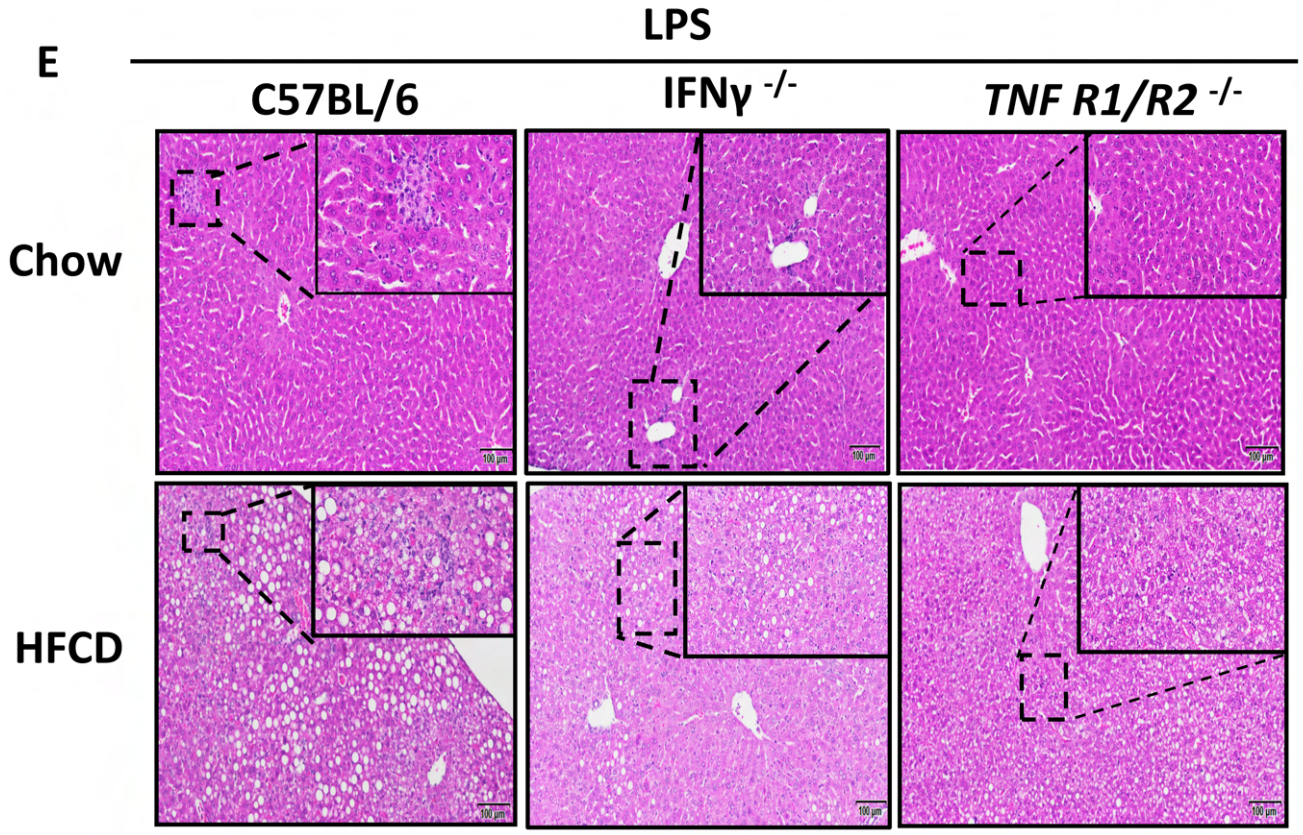
E
LPS
C57BL/6
IFNγ -/-
TNF R1/R2 -/-
Chow
HFCD

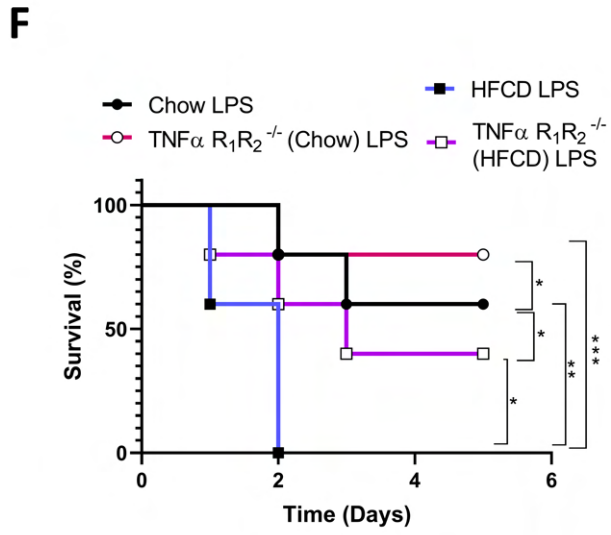
F
Chow LPS
TNFα R1R2 -/- (Chow) LPS
HFCD LPS
TNFα R1R2 -/- (HFCD) LPS
Survival (%)
100
50
0
0
2
4
6
Time (Days)
*
*
*
**
***

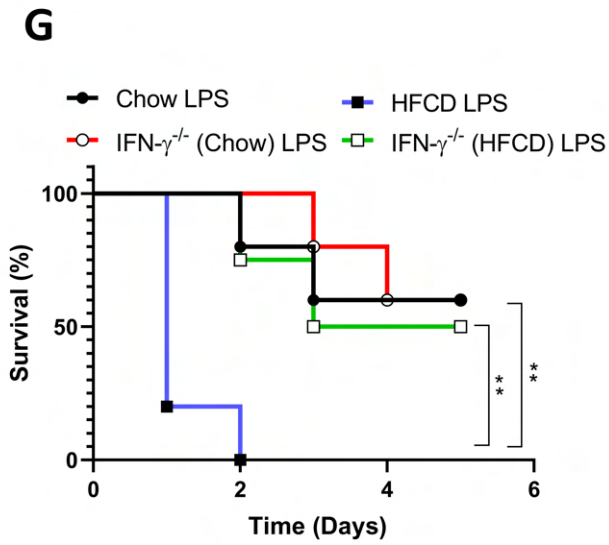
G
Chow LPS
IFN-γ -/- (Chow) LPS
HFCD LPS
IFN-γ -/- (HFCD) LPS
Survival (%)
100
50
0
0
2
4
6
Time (Days)
**
**

Figure 4

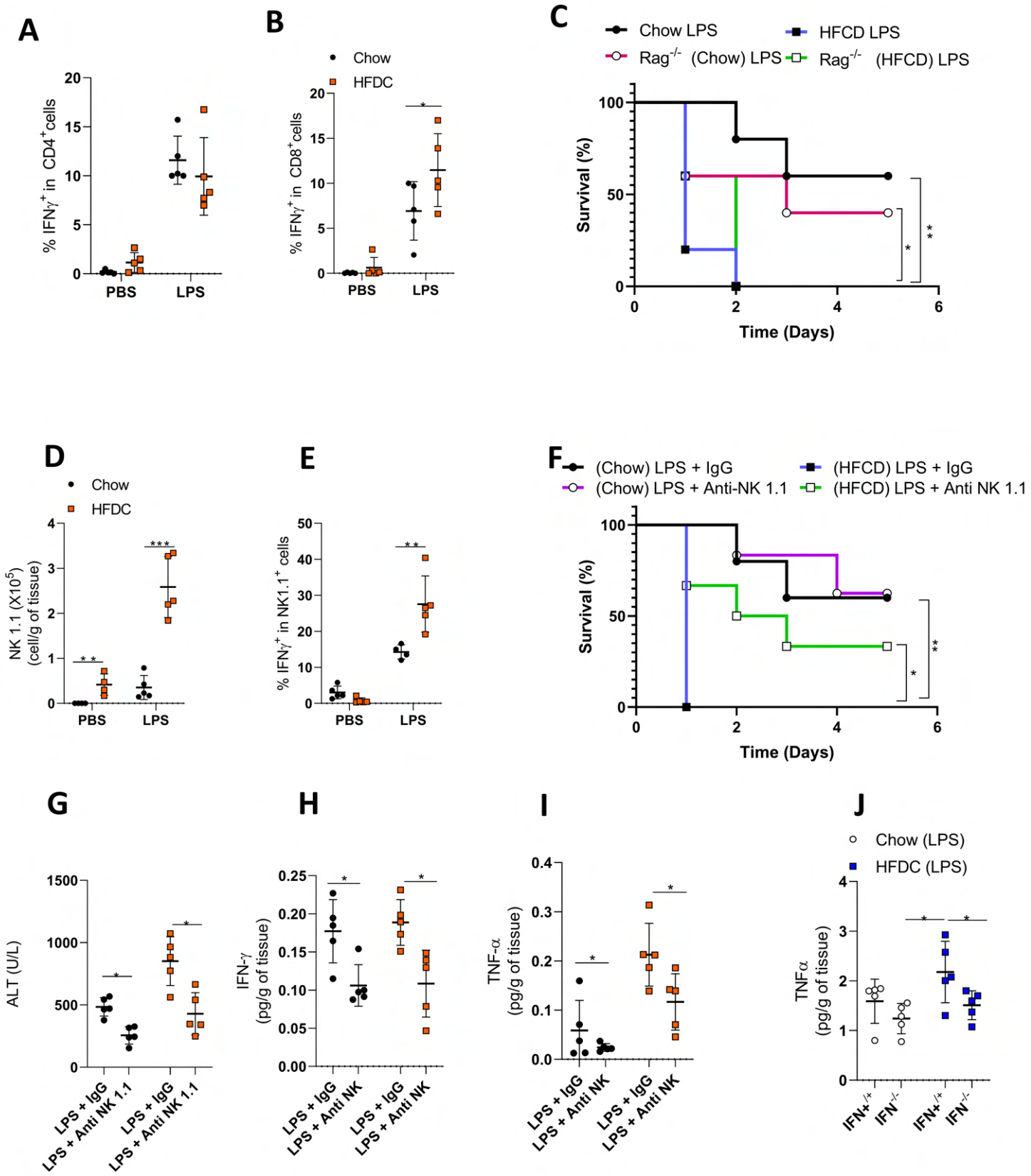
A
% IFNγ+ in CD4+cells
PBS
LPS
B
Chow
HFDC
% IFNγ+ in CD8+cells
PBS
LPS
C
Chow LPS
HFCD LPS
Rag-/- (Chow) LPS
Rag-/- (HFCD) LPS
Survival (%)
Time (Days)
D
Chow
HFDC
NK 1.1 (X10^5) (cell/g of tissue)
PBS
LPS
E
% IFNγ+ in NK1.1+ cells
PBS
LPS
F
(Chow) LPS + IgG
(HFCD) LPS + IgG
(Chow) LPS + Anti-NK 1.1
(HFCD) LPS + Anti NK 1.1
Survival (%)
Time (Days)
G
ALT (U/L)
LPS + IgG
LPS + Anti NK 1.1
H
IFN-γ (pg/g of tissue)
LPS + IgG
LPS + Anti NK
I
TNF-α (pg/g of tissue)
LPS + IgG
LPS + Anti NK
J
Chow (LPS)
HFDC (LPS)
TNFα (pg/g of tissue)
IFN+/+
IFN-/-

Figure 5

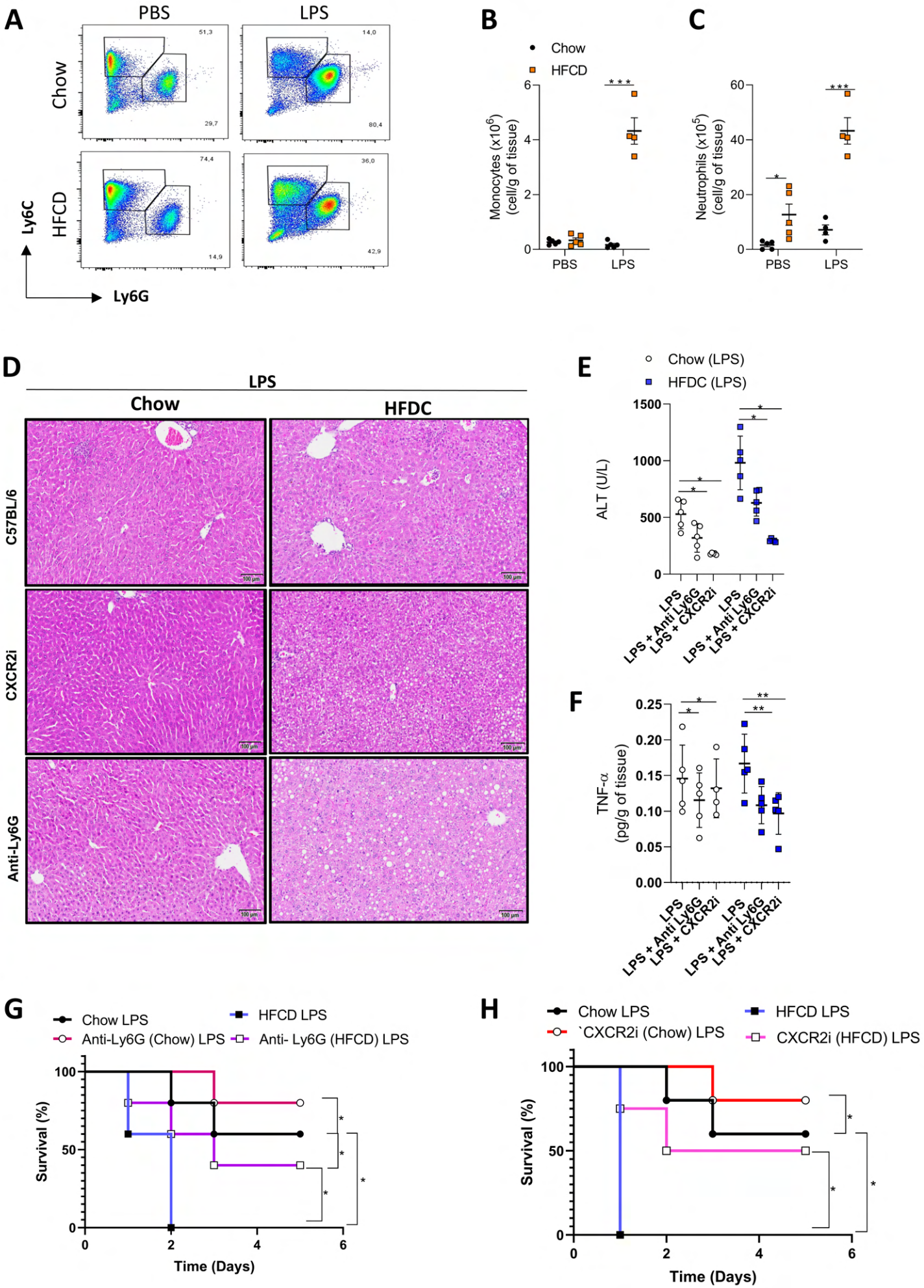
A
PBS
LPS
Chow
HFCD
Ly6C
Ly6G
51,3
29,7
14,0
80,4
74,4
14,9
36,0
42,9
B
Chow
HFCD
Monocytes (x10^6) (cell/g of tissue)
PBS
LPS
C
Neutrophils (x10^5) (cell/g of tissue)
D
LPS
Chow
HFDC
C57BL/6
CXCR2i
Anti-Ly6G
E
Chow (LPS)
HFDC (LPS)
ALT (U/L)
LPS
LPS + Anti Ly6G
LPS + CXCR2i
F
TNF-α (pg/g of tissue)
G
Chow LPS
HFCD LPS
Anti-Ly6G (Chow) LPS
Anti- Ly6G (HFCD) LPS
Survival (%)
Time (Days)
H
Chow LPS
HFCD LPS
`CXCR2i (Chow) LPS
CXCR2i (HFCD) LPS
Survival (%)
Time (Days)

Figure 6

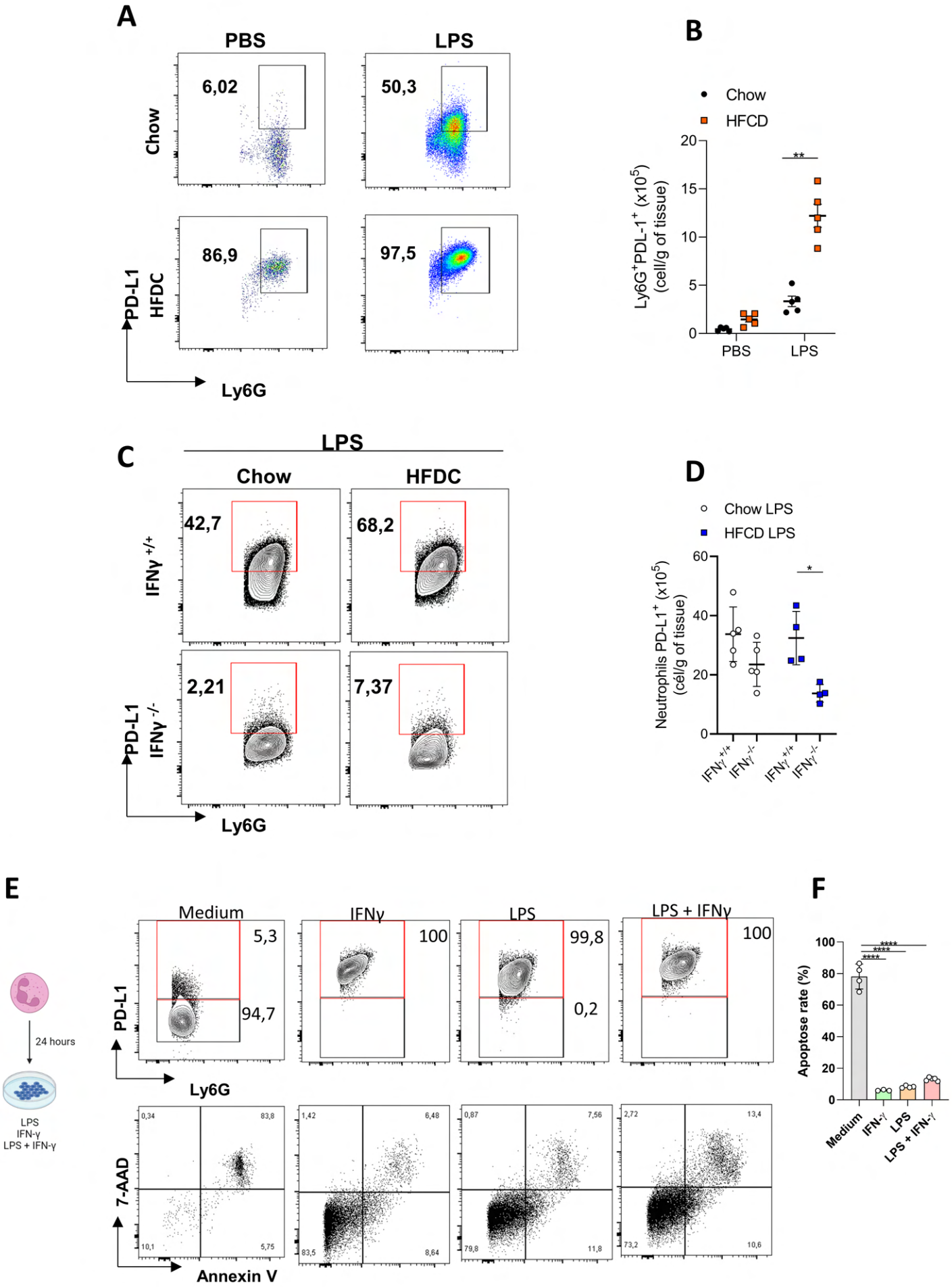
A
PBS
LPS
Chow
HFDC
PD-L1
Ly6G
6,02
50,3
86,9
97,5
B
Chow
HFCD
Ly6G+PDL-1+ (x10^5) (cell/g of tissue)
PBS
LPS
**
C
LPS
Chow
HFDC
IFNγ +/+
IFNγ -/-
42,7
68,2
2,21
7,37
D
Chow LPS
HFCD LPS
Neutrophils PD-L1+ (x10^5) (cél/g of tissue)
IFNγ+/+
IFNγ-/-
*
E
24 hours
LPS
IFN-γ
LPS + IFN-γ
Medium
IFNγ
LPS
LPS + IFNγ
5,3
94,7
100
99,8
0,2
100
7-AAD
Annexin V
F
Apoptose rate (%)
Medium
IFN-γ
LPS
LPS + IFN-γ
****

Figure 7

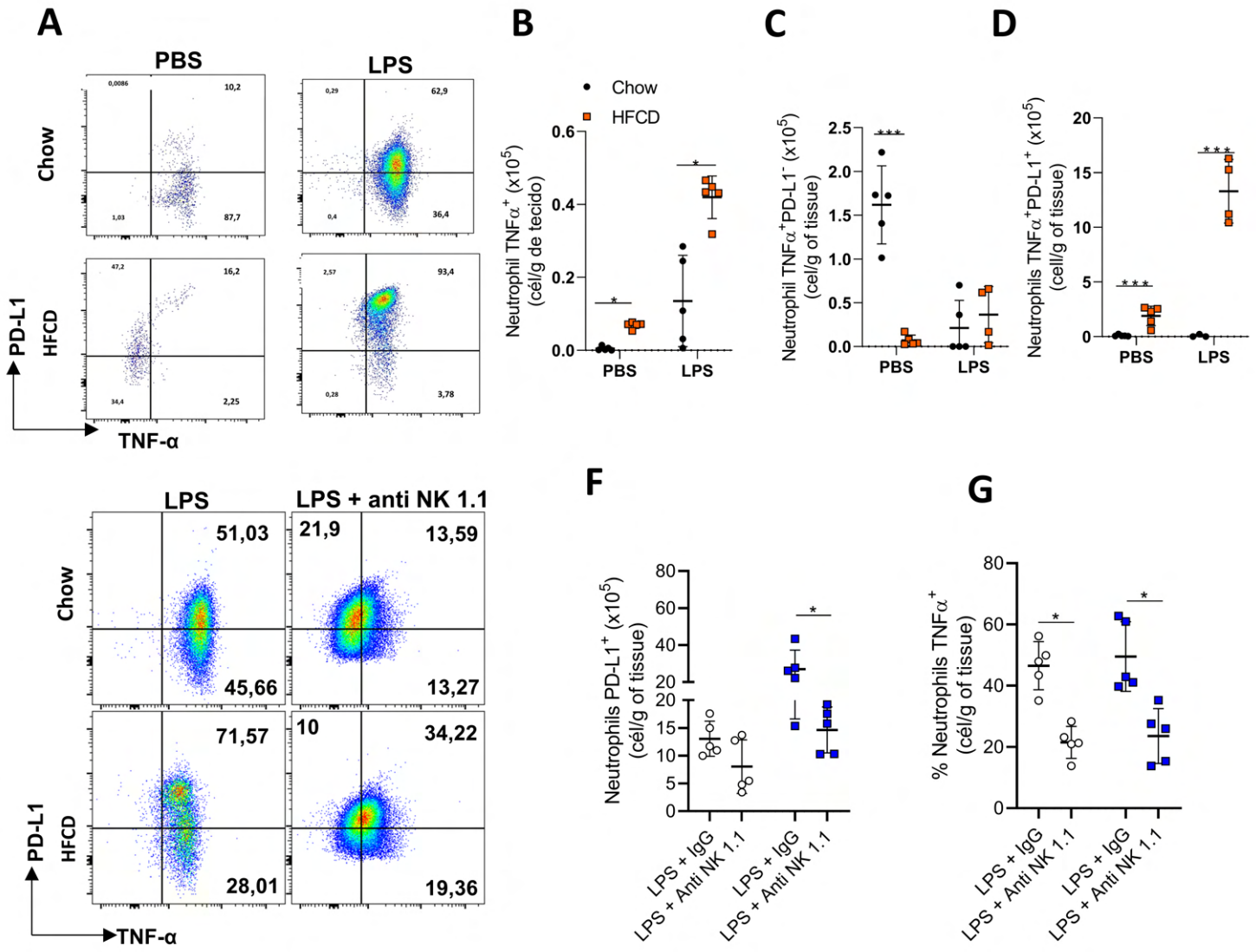
A
PBS
LPS
Chow
HFCD
PD-L1
TNF-α
0,0086
10,2
1,03
87,7
0,29
62,9
0,4
36,4
47,2
16,2
34,4
2,25
2,57
93,4
0,28
3,78
B
Chow
HFCD
Neutrophil TNFα+ (x10^5) (cél/g de tecido)
PBS
LPS
C
Neutrophil TNFα+PD-L1- (x10^5) (cel/g of tissue)
D
Neutrophils TNFα+PD-L1+ (x10^5) (cell/g of tissue)
LPS
LPS + anti NK 1.1
51,03
45,66
71,57
28,01
21,9
13,59
13,27
10
34,22
19,36
F
Neutrophils PD-L1+ (x10^5) (cél/g of tissue)
LPS + IgG
LPS + Anti NK 1.1
G
% Neutrophils TNFα+ (cél/g of tissue)

Figure 8

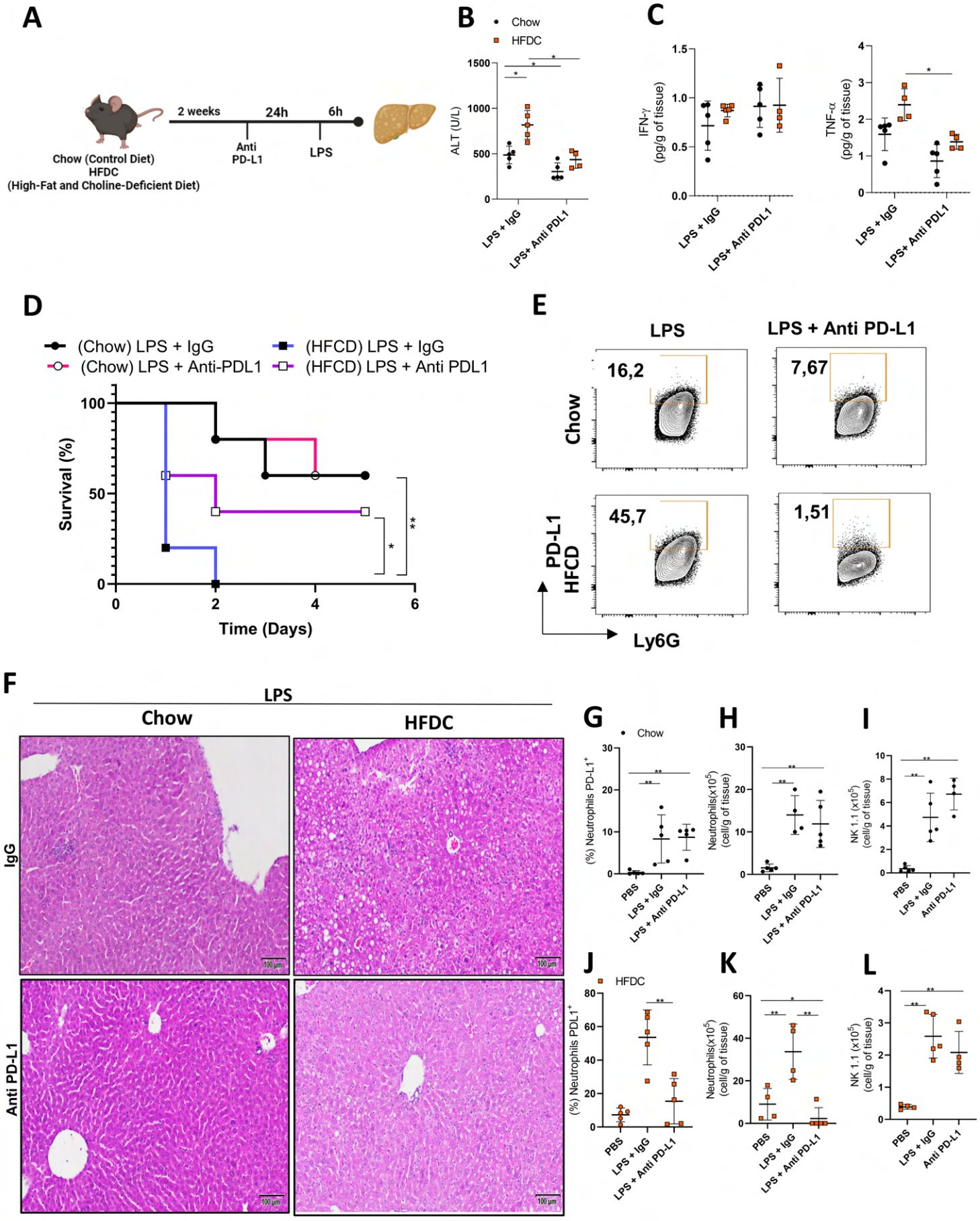
A
2 weeks
24h
6h
Anti PD-L1
LPS
Chow (Control Diet)
HFDC
(High-Fat and Choline-Deficient Diet)
B
Chow
HFDC
ALT (U/L)
LPS + IgG
LPS+ Anti PDL1
C
IFN-γ (pg/g of tissue)
TNF-α (pg/g of tissue)
D
(Chow) LPS + IgG
(Chow) LPS + Anti-PDL1
(HFCD) LPS + IgG
(HFCD) LPS + Anti PDL1
Survival (%)
Time (Days)
E
LPS
LPS + Anti PD-L1
Chow
HFCD
PD-L1
Ly6G
16,2
7,67
45,7
1,51
F
LPS
Chow
HFDC
IgG
Anti PD-L1
G
H
I
J
K
L
(%) Neutrophils PD-L1+
Neutrophils(x10^5) (cell/g of tissue)
NK 1.1 (x10^5) (cell/g of tissue)
PBS
LPS + IgG
LPS + Anti PD-L1
Anti PD-L1